Multi-robot System for Autonomous Cooperative Counter-UAS Missions: Design, Integration, and Field Testing

Antonella Barisic¹, Marlan Ball², Noah Jackson², Riley McCarthy², Nasib Naimi³, Luca Strässle³, Jonathan Becker³, Maurice Brunner³, Julius Fricke³, Lovro Markovic¹, Isaac Seslar⁴, David Novick⁴, Jonathan Salton⁴, Roland Siegwart³, Stjepan Bogdan¹, and Rafael Fierro²

Abstract—With the rapid development of technology and the proliferation of uncrewed aerial systems (UAS), there is an immediate need for security solutions. Toward this end, we propose the use of a multi-robot system for autonomous and cooperative counter-UAS missions. In this paper, we present the design of the hardware and software components of different complementary robotic platforms: a mobile uncrewed ground vehicle (UGV) equipped with a LiDAR sensor, an uncrewed aerial vehicle (UAV) with a gimbal-mounted stereo camera for air-to-air inspections, and a UAV with a capture mechanism equipped with radars and camera. Our proposed system features 1) scalability to larger areas due to the distributed approach and online processing, 2) long-term cooperative missions, and 3) complementary multimodal perception for the detection of multirotor UAVs. In field experiments, we demonstrate the integration of all subsystems in accomplishing a counter-UAS task within an unstructured environment. The obtained results confirm the promising direction of using multirobot and multi-modal systems for C-UAS.

I. INTRODUCTION

The capabilities, speed, size, and widespread use of small uncrewed aerial vehicles (UAVs) [1] offer countless opportunities for their beneficial use [2]. Nevertheless, they also present a security concern that must be addressed. Intruders of protected airspace, i.e., airborne UAVs that are not authorized to be in the airspace, must be countered in a safe and noninvasive manner in order to protect the area of interest, especially when public safety is at risk. Typical venues, where counter-UAS (C-UAS) systems would help ensure safety, include public gathering places, airports, hospitals, power plants, prisons, and so forth [3], [4].

This work was supported by NATO Science for Peace and Security Programme.

¹Antonella Barisic, Lovro Markovic, and Stjepan Bogdan are with the Laboratory for Robotics and Intelligent Control Systems (LARICS), Faculty of Electrical Engineering and Computing, University of Zagreb, 10000 Zagreb, Croatia. Please direct all correspondence to antonella.barisic@fer.hr

²Marlan Ball, Noah Jackson, Riley McCarthy, and Rafael Fierro are with the Electrical and Computer Engineering Department, University of New Mexico, Albuquerque, NM 87131, USA

³ Nasib Naimi, Luca Strässle, Jonathan Becker, Maurice Brunner, Julius Fricke, and Roland Siegwart are with Autonomous Systems Lab (ASL), ETH Zurich, 8092 Zurich, Switzerland

⁴Isaac Seslar, David Novick, and Jonathan Salton are with Sandia National Laboratories, Albuquerque, New Mexico, 87185, USA, a multimission laboratory managed and operated by National Technology and Engineering Solutions of Sandia, LLC., a wholly owned subsidiary of Honeywell International, Inc., for the U.S. Department of Energy's National Nuclear Security Administration under contract DE-NA0003525.

Sand Number: SAND2022-9903 C

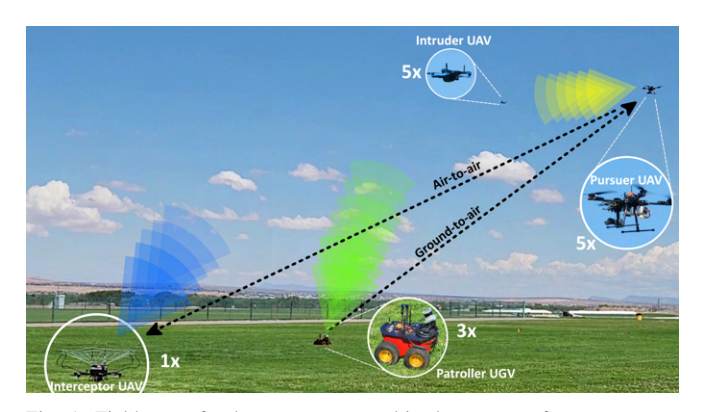


Fig. 1: Field test of a heterogeneous multi-robot system for autonomous cooperative C-UAS missions. In this version of the pursuit-evasion game, agents cooperate in ground-to-air and air-to-air missions. Each agent, the patroller UGV, the pursuer UAV, and the interceptor UAV have their sensors and estimators that together provide a multimodal perception of the intruder UAV

Potential intruders, especially multirotor vehicles, have a small cross-section and are difficult to detect reliably with purely ground-based systems (e.g., radar or electro-optical). Ground-based sensors are static and suffer from interference with the earth, vegetation, and other structures that obscure objects at low altitudes. Adding sensors to mobile UAV platforms improves detection accuracy and reliability by bringing onboard sensors closer to the target while reducing the signal-to-noise ratio. This is the idea behind the international collaborative project Mobile Adaptive/Reactive Counter UAS System (MARCUS), which combines complementary robotic platforms on the ground and in the air to form a cooperative autonomous multi-robot system, as shown in Fig. 1. By working together and sharing information to accomplish a specific task, multi-robots demonstrate better performance and are more robust, reliable, and go beyond the efforts of individual robots. Therefore, the proposed MARCUS framework provides an innovative solution to this global problem and includes three main elements: (i) detection, (ii) tracking, and (iii) mitigation of the intruder with no or little collateral damage. In addition to using multiple different robotic platforms to complement their advantages and create a long-term energy-efficient system, we also develop a multimodal perception to detect and localize potential intruders. Multimodal sensing exhibits superior performance compared to uni-modal by being more information-dense, more robust to changes in dynamic and unstructured environments, and ultimately more accurate and reliable.

This paper reports the detailed design and development

of the robotic platforms, the integration of subsystems and various sensing modalities, and reports the results of field tests that confirm a reliable and robust solution to ensure the safety of the airspace. The remainder of the paper is organized as follows: Section II formulates the problem of the pursuit-evasion game, while Section III describes the technical details of the design and construction of the robotic platforms applied in the proposed framework. Section IV describes multimodal perception in detail, along with a brief description of the high-level control algorithms. Section V presents the findings and results of the field tests and the fully integrated end-to-end mission.

A. Related Work

Out of concern for public safety, national security and individual privacy [3], the C-UAS problem has been addressed through several approaches, with ground-based solutions still being the predominant application. Vision-based UAV detection and classification have been addressed in [5], [6], [7], [8], [9]. A novel approach to generate a synthetic aerial dataset for UAV detection, considering the imaging conditions specific for air-to-air, namely long-range detection and detection under changing illumination, is developed in [10]. Other sensing technologies commonly used by C-UAS include radio frequency (RF) [11], acoustic, optical (IR), LiDAR [12], and radar (3 MHz - 300 GHz) [13]. While most air-based solutions assume that early detection of the intruder is done by an external system [14], [15] and have limited deployment duration due to limited flight time [5], [6], [7], [8], [9], [16], we present a complete long-term endto-end solution from initial ground-based detection to air-toair inspection and mitigation.

In our previous work, we proposed an air-to-air approach focusing on the tracking component. Using stochastic reachability, we demonstrate a globally optimal solution to the path planning problem of a single pursuer in pursuit of a non-adversarial stochastic target [15]. A similar indoor approach is described in [16] where a pursuer UAV autonomously detects and tracks a small UAV in a GPS-denied environment. Once a small UAV has been identified as a threat by the counter system, the next step is mitigation, which can include various measures such as warning, control, disruption, disabling, and destruction. These actions are executed by various mitigators or interceptors such as [4],

- a) Nonphysical: RF/GNSS jamming, spoofing, high-power microwaves, and lasers.
- b) Physical: Nets, projectiles, collision UAVs, and eagles.

As MARCUS' goal is neutralizing a micro UAV with minimal or no collateral damage, it utilizes an *air-to-air* interception method described in Section IV-C. Specifically, MARCUS integrates a unique and autonomous flying net capable of safely capturing micro UAVs. Catching drones with nets are discussed in [17], [18], [19]. The authors in [20] used a cylindrical net with a large cross-section at any angle of approach by combining it with a predictive control law for air-to-air interception.

Finally, a novel bio-inspired interception approach that can be leveraged for C-UAS is described in [21], [22]. Also, swarm-based and multi-drone neutralization systems, as described in this paper and in [23], [13], [24], can take advantage of cooperative sensing, team coordination, deployment flexibility, and robustness. However, in contrast to the above approaches, we cross the boundaries from simulation and theory to real-world deployment and report our results and findings on integration and field testing.

II. PROBLEM FORMULATION AND PRELIMINARIES

The problem addressed in this paper is a complex variant of the pursuit-evasion game (PEG), as shown in Fig. 1. Our system consists of five types of agents: target, intruder, patroller, pursuer, and interceptor. The target in this PEG is not the robot, but the center of the protected area, which makes it a target-guarding problem. The intruder is an unknown multirotor aerial vehicle that enters protected airspace. The intruder is non-cooperative but its intent is unknown, as it could be a stray vehicle or a threat. The patroller is a ground vehicle equipped with a sensing system for long-term patrols over the protected area. The second agent capable of sensing the intruder is the pursuer, a UAV for air-to-air inspection and verification of a possible intruder. Finally, the interceptor is a UAV for fast and safe interception of the intruder. The complexity of the presented problem arises not only from the number of different agents and their roles but also from the need for cooperation between the agents.

Our scenario takes place in a predefined region of interest, as shown in Fig. 4. The number of agents of each type can be scaled to achieve the desired coverage. Each agent type has a unique role in mission accomplishment. They complement each other to provide the best coverage and sensing by taking into account operating time and efficiency. The operating time of the developed robotic platforms is given in Table I. In concert, the proposed system can be used for long-term deployments with minimal maintenance and intervention. The developed framework can handle an unlimited number of intruders over time but assumes one intruder at a time. To deal with multiple intruders at once, the system can be scaled to include more interceptors and pursuer UAVs, with each pursuer-interceptor pair able to mitigate one intruder at a time. The intruder belongs to the classification of micro multirotor UAVs with a wingspan of less than 50 cm [25] and a weight of less than 2 kg [26] making it difficult to detect by sensor technologies.

TABLE I: Operating time of robots developed for the MARCUS project.

Agent	Patroller UGV	Pursuer UAV	Interceptor UAV
Operating time	10 hours	25 mins	10 mins

III. HETEROGENEOUS MULTI-ROBOT SYSTEM

In this section, we present details of cooperative autonomous robots in our heterogeneous framework. Each robot is equipped with a different set of sensors to take full advantage of the specific platform. The presented robots use the Robot Operating System (ROS) as middleware, which

is the basis for the interoperability of our system. Details of the hardware components and low-level control are presented below.

A. UGV for Long-term Patrols

In the framework developed for the MARCUS project, the patroller agent is implemented using a mobile UGV platform. The goal of the patroller is to operate over long periods and perform initial detection of potential intruders. We selected the Pioneer 3-AT, a mobile platform with two motors on each side connected with timing belts, allowing skid-steer, all-terrain operation. The Pioneer is controlled by Pixhawk running ArduRover autopilot software, and Jetson Xavier NX as the onboard computer. The patroller is equipped with an Ouster OS0-128 LiDAR mounted on a Directed Perception Pan-Tilt Unit (PTU). The LiDAR has 128 beams with a 90-degree vertical field of view (FOV) and 2048 readings at 10Hz in each 360-degree scan. The UGV is powered by 5 separate batteries that provide long-term operation in the range of 10 hours.

B. UAV for Inspection and Verification

The pursuer UAV is a mid-sized quadrotor with full onboard computation, designed and built specifically for the MARCUS project. It has a 91 cm wingspan and is controlled by a Pixhawk Cube Orange flight controller equipped with a full sensor suite and Arducopter software. The full autonomy software stack runs on the NVIDIA Jetson Xavier NX. The Jetson receives stereo image data from a Stereolabs Zed Mini camera mounted on a custom two-axis gimbal being stabilized by two servo motors. The pursuer UAV has a flight time of about 25 minutes and can reach speeds of more than 95 kilometers per hour.

C. UAV for Interception

For the safe mitigation of an intruder, a custom hexacopter UAV was built with a specialized catching mechanism. A catching mechanism is mounted on the top of the UAV, consisting of a structural net to transfer the energy of the impact to its six arms made from carbon fiber, which were designed to absorb the impact optimally. On top of the structural net, there is a second, thinner net that entangles the propellers of the intruder UAV during a catch. Point clouds generated by two Texas Instruments AWR1843AOP millimeter-wave radars in different configurations and images from a Flir Chameleon3 color camera are processed by the onboard computer, an NVIDIA Jetson Xavier NX. The sensors and computing unit are protected by a 3D-printed dome covered with plexiglass. The whole system allows for a flight time of approximately 10 minutes.

D. Ground Station

A cooperative mission of our multi-robot system is monitored via a graphical user interface (GUI), as shown in Fig. 2. The presented GUI is tailored for C-UAS operation, but is generally used for various operations of multiple UAVs, as explained in [2]. A human operator can track the state

of each robot (e.g., idle, tracking, or approach) and observe their GPS locations on a preloaded offline map. Since all algorithms are computed online, the robots report only the most relevant information to the ground station. The final output of the sensing algorithms is transmitted to the ground station and displayed on the map as the GPS location of the detected intruder.



Fig. 2: Graphical user interface for multi-robot cooperative C-UAS operation

The developed system can operate fully autonomously or follow a human-in-the-loop (HITL) approach. The difference lies in two points of human interaction that serve as an additional layer of safety when the agents interact. The human operator can only confirm or deny the transition to the next robot in the mission. To make an informed decision, our GUI provides the cropped RGB image of the detected intruder which is transmitted from the pursuer UAV. The visual detection of the intruder provides rich data and is the most important aspect of human-machine interaction provided by our GUI. In our experiments, we use the HITL approach, and this would most likely also be the case in industrial applications due to safety and regulatory requirements there. This feature can be turned off by disabling the two human interaction points for a fully autonomous mission.

IV. SENSING AND MITIGATION

In this section, we describe three principal components of C-UAS: detection, tracking, and mitigation. Detection refers to processing sensor data and analyzing it to extract valuable information, such as whether an intruder is in a protected area and where it is located. Each of our robots has this component and is based on different sensor data. In this way, we take advantage of different sensor modalities to increase the probability of detecting possible intruders. The next step is to track the intruder over a longer time to get a better insight into its intentions and the necessary information to plan future actions. Once we have all this, we proceed to mitigation by safely removing the risk while ensuring no or minimal damage. The overall software architecture and data flow are visualized in Fig. 3, while a detailed description is given in the following subsections.

A. LiDAR-based Detection

Initial detection of intruders is accomplished by analyzing point clouds from a LiDAR sensor mounted on a pan-tilt

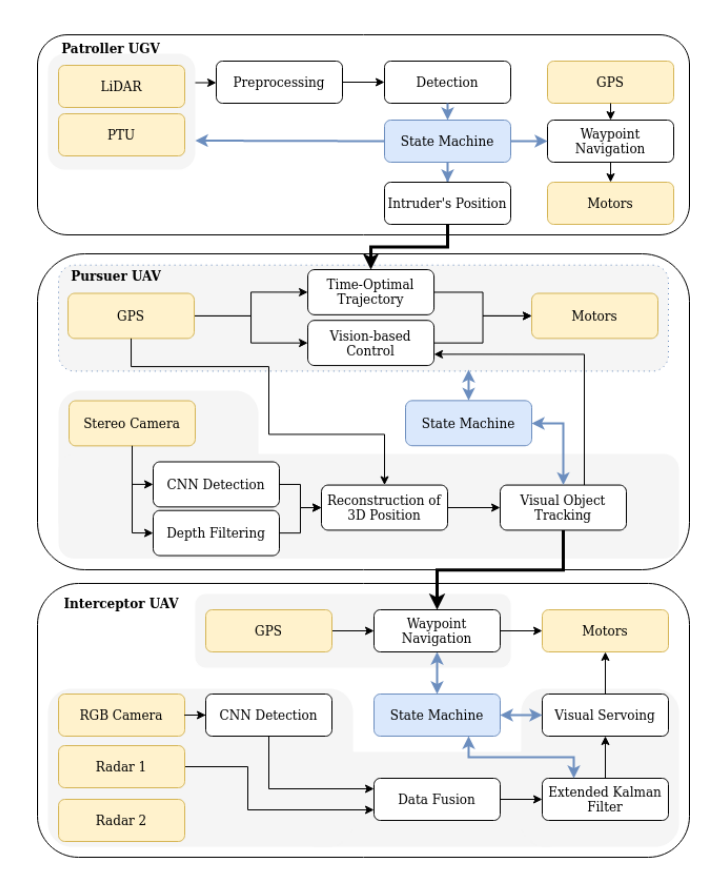


Fig. 3: Overview of the software architecture and data flow for a cooperative robotic system with multi-modal perception. The yellow color highlights the sensors and the blue color highlights the decision part of the system. Only the most important components are shown.

unit (PTU). The patroller runs a waypoint mission on the outer boundaries of the protected area, as shown in Fig. 4. The patroller stops at each waypoint to scan and search for possible intruders. The Ouster OS0-128 has a vertical angular resolution of 0.7°, resulting in a vertical distance between two beams of 61cm at a distance of 50m, which is the maximum range reported by the manufacturer. This gap provides enough space for micro UAVs to avoid detection. For this reason, we constantly tilt the LiDAR sensor during the scanning phase using the PTU.



Fig. 4: Waypoint mission of the patroller UGV equipped with LiDAR sensor.

We narrow the azimuth window of the LiDAR to 120° to reduce the amount of data to be processed. We also increase the signal strength to 3x to improve the detection

probability. The other parameters of the sensor are set to default values. The first step is to preprocess the point cloud to filter out data that is outside of our protected airspace. On the filtered point cloud, we detect intruders by applying the Euclidean clustering algorithm. The output clusters are considered candidates for further inspection by the pursuer UAV. To transform the cluster detections into GPS data, we define three coordinate frames: a global frame L_G , a patroller's body frame L_B , and a sensor frame L_S . The 3D position of detected intruder in sensor frame (LiDAR mounted on a PTU unit) is $\mathbf{p}_i^S = (x_i, y_i, z_i)$. Based on the rotation data obtained from the PTU encoders and known translation, we define the transformation matrix \mathbf{T}_{B}^{S} from frame L_S to frame L_B to obtain the intruder's position in the body frame $\mathbf{p}_i^B = \mathbf{T}_B^S \mathbf{p}_i^S$. The patroller's pose in the global frame is computed by the on-board localization sensors and can be written as a transformation matrix \mathbf{T}_G^B . Finally, the detected intruder's position in the global frame is:

$$\mathbf{p}_i^B = \mathbf{T}_G^B \mathbf{T}_R^S \mathbf{p}_i^S, \tag{1}$$

which is then converted to GPS coordinates by knowing the GPS position of L_G origin, and reported to the pursuer UAV and graphical interface.

B. Vision-based Detection and Tracking

Upon successful detection by the LiDAR sensor, the pursuer UAV starts its mission and begins the search, which is accomplished by a time-optimal trajectory [27]. The trajectory is in the form of a spiral, oriented towards the reported location and narrowing inward (see Fig. 5). The position reported by LiDAR is only used to cue the pursuer UAV to an approximate location, as it has its detection system for a more detailed investigation. Searching over a larger area and then moving closer to the reported location increases the likelihood of detecting the intruder even if it changes position, which is very likely. During the search, the convolutional neural network (CNN) processes the right image of the stereo pair. In this work, we deploy YOLOv4 Tiny trained on the synthetic dataset described in [10] and fine-tuned it on a smaller subset of real images.

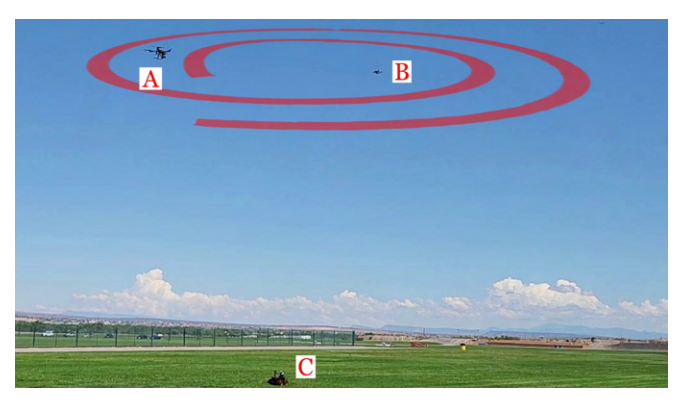


Fig. 5: The pursuer UAV (A) in spiral search for the intruder (B) after receiving initial detection from the patroller UGV (C).

If an intruder is detected, we filter the depth data based on the techniques described in [6] to remove noise and ensure reliable measurements for control. As shown in Fig. 3, the output of CNN detection and depth filtering is then used to reconstruct the 3D position of the intruder using the pinhole camera model. The linear Kalman filter with the constant velocity model is then used for visual object tracking (VOT). The output of VOT is fed to the positionbased visual servoing to navigate the pursuer towards the intruder. Our goal is to keep the intruder in the center of the image, slightly above the horizon and at a certain distance. The distance is determined empirically (6 m) as a tradeoff between having enough space for UAV maneuvers without collisions and obtaining reliable sensor readings (which correlate with distance). Based on the sensor inputs and the data received from the other robots, the state of the pursuer is controlled by a finite state machine. The pursuer UAV sends the GPS location of the intruder to the interceptor UAV in response to the request to intercept it and waits for the interceptor to respond that it is approaching for safe mitigation.

C. Mitigation

The interceptor autonomously takes off and moves below the received GPS position, where the images of the upwarddirected camera are processed by a CNN based on YoloV4 Tiny architecture, similar to the one mentioned in Section IV-B. This model was trained to detect multirotors in an overexposed sky from below the intruder UAV looking upwards. Furthermore, the two radars search for any objects in their field of view. Upon detection of the intruder by both image and radars, an Extended Kalman filter with a constant velocity model estimates the relative 3D position and velocity of the intruder. It uses pre-filtered image coordinates and derivatives from the detection, a pre-filtered distance given by the radars, and IMU data to model the egomotion of the interceptor. The planner takes the estimate of the intruder's position as an input to its policy with the following goals: keeping the intruder in the center of the sensor's field of view, maintaining zero relative horizontal velocity, and ensuring that a given following distance is held to the target. The planner then outputs body rate and thrust commands which are fed to the UAV's flight controller. Once the interceptor is following the intruder safely and the operator has requested a catch, the planner reduces its distance to the intruder whilst maintaining it in the center of the field of view and keeping the relative horizontal velocity at zero. Finally, once the relative distance is small enough, a last high thrust command is sent to capture the intruder by entangling the propellers in the net, thus neutralizing the intruder without damaging it. Once the catch has been completed, the interceptor safely returns to a predesignated location, with the intruder secured in its net.

V. FIELD EXPERIMENTS

In parallel with the development of the hardware, the software components were tested in the ROS-compatible physics simulator called Gazebo. Each robotic platform and its sensor module were developed independently. After the

initial development in simulation, a series of extensive field experiments were conducted to test each software component and robotic platform. Integration of the entire system was performed in the field. In the following, we report the results of the field experiments and the integration of the developed system.

A. Ground-to-air Sensing

The first objective of our mission is to patrol the area and constantly scan in search of potential intruders to ensure secure airspace. We define an area of interest and plan a waypoint mission on its boundaries, as seen in Fig. 4, to provide better coverage as the probability of detection decreases with the distance from the sensor. We run multiple experiments with the described setup using Skydio 2+ as an intruder (wingspan of 30 cm) and draw some conclusions.

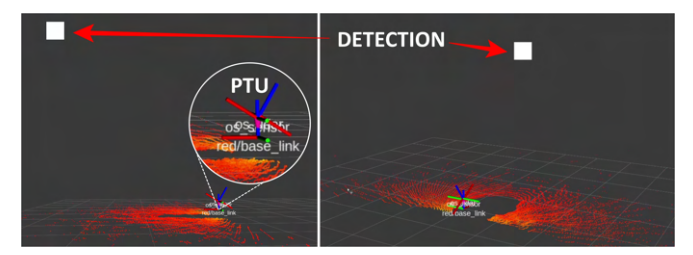


Fig. 6: Detection of the intruder in the point cloud data received from the LiDAR sensor mounted on the PTU. The white square indicates a positive detection.

In general, LiDAR scans provide a large amount of highprecision data, but sparse data, which is especially evident when the objects in the scene are small or farther away from the sensor. This is the case with C-UAS systems which must be able to detect micro UAVs (with a wingspan of less than 50 cm [25]). To compensate for the gaps between laser beams at a given location, the ground-based LiDAR constantly tilts and scans at different angles. In the field experiments presented in Table II, where the intruder hovers in place, we show that tilting leads to more detection hits at longer distances from the target (Experiments 1 through 3). By moving the LiDAR sensor with the PTU unit, we overcome the problem of gaps between beams and effectively increase the detection range for small objects. At shorter distances (experiment 4), no tilting leads to more hits, as the detection hits line up quickly. In Fig. 6, we can see that the PTU unit with the mounted Ouster sensor is tilted with respect to the base of the patroller UGV, while the point cloud data is transformed into the body frame of the robot. Since we have only one class of objects and assume that everything in the airspace is either known in advance or is a potential candidate for closer inspection, each output of the clustering is a candidate for the pursuer UAV.

Another important aspect of LiDAR-based detection is the reflectivity of an object's surface material. We tested two different materials in outdoor environment, one is matte plastic and the other is aluminum. As expected based on the reflectivity properties of these materials, matte plastic shows lower reflectivity and reduces the likelihood of detection,

TABLE II: Effect of LiDAR sensor tilting on detection range and number of detection hits.

Expt. No.	Tilting	No. of detections	Distance to intruder[m]	
1	Yes	26	20.6782	
	No	14		
2	Yes	434	21.1131	
2	No	2	21.1131	
3	Yes	322	21.1033	
	No	0	21.1033	
4	Yes	25	6.0727	
	No	225	6.9727	

while aluminum material shows high reflectivity. Since the accuracy of LiDAR-based detection depends on the material properties of the intruder, it is advantageous to couple LiDAR with another modality that is independent of it.

B. Air-to-air Inspection

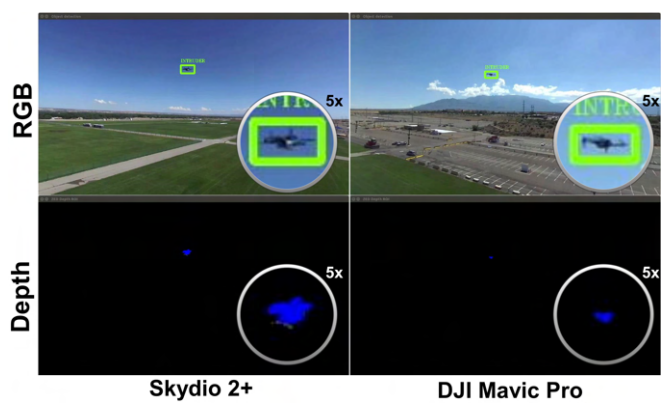


Fig. 7: RGB-D detection from the stereo camera onboard the pursuer UAV. The top row shows the CNN-based detection, and the bottom row shows the filtered depth image where the blue pixels represent the selected depth measurements. For both experiments, we use micro UAVs: the Skydio 2+ on the left and the DJI Mavic Pro on the right.

To complement the sparse and accurate detections from the ground-based LiDAR sensor, the pursuer UAV is utilizing a stereo camera. The stereo camera provides dense RGB-D data at a shorter range and requires high computational resources to provide accurate depth measurements. The depth sensing range is 12 m. By using a shape-based object representation achieved with synthetically generated data, we can detect the shape of the intruder from very far away, resulting in only a few pixels in the image. The detector is capable of detecting micro UAVs up to a distance of about 30 m, at which moment the intruder occupies only 0.01% of the pixels in the image. If the intruder leaves the camera's field-of-view or is too far away to be detected, we can redetect it again and continue visual tracking, as shown in Fig. 8.

Based on extensive experiments (more than 15 hours of autonomous flight time), we report that the pursuer UAV can track and follow the intruder moving at up to 2 m/s with a 100% success rate, regardless of whether the intruder is either moving away, moving toward it or simply hovering. At higher speeds, our pursuer can track the receding intruder in most cases (tested at 4 m/s), but when the intruder moves

toward the pursuer, the pursuer tries to avoid a collision and thus usually loses sight of the intruder. Besides repeatability, the other important feature of air-to-air inspection is the generalization of different possible UAV models. In the conducted experiments, we alternately use Skydio 2+ and DJI Mavic Pro as intruders. As can be seen in Fig. 7, the developed system can detect, inspect, and track the two mentioned micro UAVs.

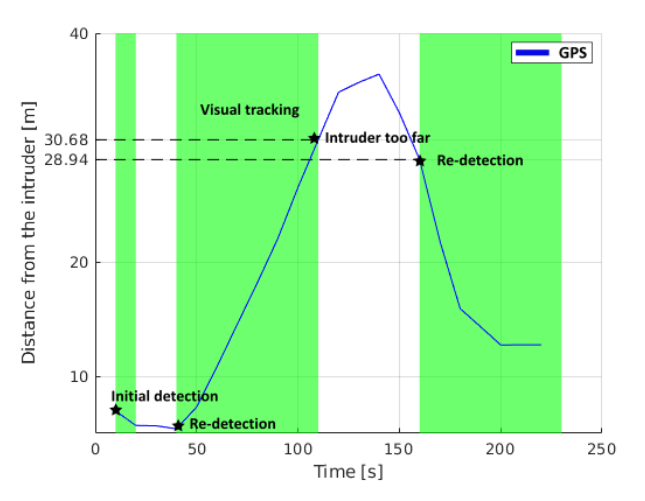


Fig. 8: Visual detection as a function of distance from the intruder. The blue line is the ground-truth distance between the pursuer and the intruder UAV, measured from GPS. The green areas denote confident visual detection and tracking. We designed the experiment to show detection over range, and re-detection in case the intruder leaves the field of view and moves too far away. Initially, the intruder is detected at a short distance (first green area), and then it leaves the field of view, causing the tracking to stop. When the intruder re-enters the field of view, the tracking continues. The intruder then moves away from the pursuer UAV, and our system continuously tracks the intruder in the image space by exploiting spatial and temporal information. At a distance of about 30 m, it is no longer possible to track the intruder. Then the intruder starts coming back, and we re-detect him again at almost the same distance as last seen.

C. Mitigation

The refined estimate of the intruder's GPS position is used by the interceptor UAV to fly autonomously to a position where it can detect and track the target on its own. Once this is the case the interceptor only relies on its two radars, the color camera, and IMU to plan body rate and thrust outputs in a local frame. GPS is only used for geofencing. This makes the system robust against GPS drift since the critical part of following and catching the intruder UAV is independent of GPS and a drift of a few meters is acceptable for geofencing as well as for flying below the estimated intruder's GPS position. Detection on the RGB data produces a reliable 2D position up to a distance of 30 meters at a rate of 35Hz for a micro UAV of 30 cm in size.

For the follow and catch maneuvers where the relative distance goes from more than ten meters to zero meters in a short time, an exact distance estimate is needed from a sensor that can handle different as well as changing distances. A single radar can only be in a given configuration, in this case, a short-range or a long-range configuration. Using two radars, one in each configuration, enables a longer range

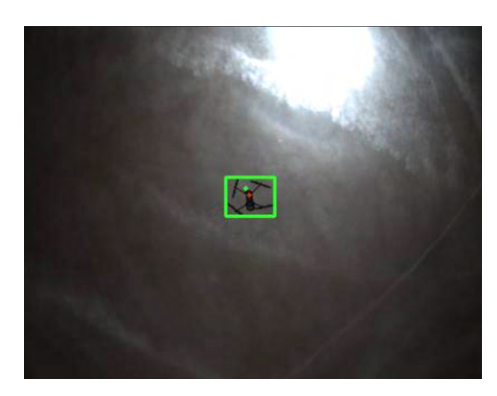


Fig. 9: Image detection of DJI Mavic Pro. The output of the detection module is depicted in green with a bounding box and the dot representing the intruder's position estimated by the radars. The red dot is the combined estimate after being filtered by the extended Kalman filter.

and better measurement resolution over the entire combined range. This double-radar setup can detect a micro UAV like the DJI Mavic Pro from a distance of half a meter up to a distance of fourteen meters. In Fig. 9 one can find an example of detection output and a filtered 2D estimate of the intruder UAV. In field tests, this setup was able to follow a DJI Mavic Pro and a Skydio 2+ flying linear and circular trajectories at non-constant speeds whilst keeping a relative distance of seven meters. In eight tests a hovering intruder UAV was successfully caught seven times without causing any additional damage to it.

D. End-to-end Mission

In this section, we report the results of an end-to-end mission of a heterogeneous cooperative multi-robot system with multi-modal sensing. In preparation for the full cooperative mission, partial integrations were also performed, from patroller UGV to pursuer UAV and from pursuer UAV to interceptor UAV. In the full mission, three different robots operate autonomously and in a distributed manner, cooperating by sharing only essential information. The trajectories of the successful end-to-end mission are shown in Fig. 10. The trajectories of the cooperative robots are reported by GPS, while the trajectory of the intruder is detected by LiDAR and a stereo camera. As described earlier, the patroller monitored the area of interest and, once it detected a potential intruder, called the pursuer UAV for closer inspection and to provide visual feedback to the ground station. The pursuer UAV approached starting position, planned the search trajectory around the reported position, and began searching. As demonstrated in this experiment, the intruder moved during the transition from ground to air sensing. Our system was able to account for this and successfully detect the intruder's new position. The pursuer continuously tracked the intruder and waited for confirmation to proceed. When the operator confirmed from the ground station that the intruder posed a potential risk, the interceptor UAV was deployed to safely retrieve the intruder. The interceptor approached the last known position of the hovering intruder and refined the position information using the fusion of radar and camera measurements. Finally, the interceptor UAV successfully and safely caught the intruder. The video of field

integration and tests is available at https://youtu.be/ ckgf-vwzany.

E. Discussion

Our results show that the synergy of different robots and sensor technologies in C-UAS solutions is a promising direction to achieve a scalable and long-term solution with multiple layers of detection technology. While previous research has focused on single-platform C-UAS solutions, we have explored the possibilities of multi-robot systems where each agent is specialized in a particular task. The results show that the developed system can be used for long-term missions (see Table I), which is not possible in solutions with only one defender UAV. Another important aspect of the developed solution is the safe mitigation of intruders, which is usually not the case with physical mitigators [4].

For flying objects in protected airspace that are not intruders, such as birds or kites, LiDAR-based detection would not be able to distinguish them from intruders. The visionbased detection algorithm, on the other hand, can distinguish multirotor UAVs from other flying objects. The greater the distance to the object, the more difficult the problem becomes as the visual features are less visible. In contrast to the situation described above, LiDAR performs better than a camera in low-light conditions. This confirms that coupling different sensors for the same task improves robustness as they complement each other. LiDAR-based detection is not common in C-UAS solutions because the cross-section of the intruders is very small, resulting in sparse LiDAR data. We address this problem by two measures: We constantly move the sensor to compensate for the gaps between the laser beams, and we use a mobile platform instead of a static one to increase the chance of getting closer to the intruder by patrolling. One of the limitations of our system is the range and resolution of the LiDAR sensor. Therefore, other types of LiDAR sensors with higher vertical angular resolution should be investigated, and the lower vertical field of view could be compensated with our approach of mounting the LiDAR on the PTU.

VI. CONCLUSION AND FUTURE WORK

In this work, we demonstrated the capabilities of a heterogeneous multi-robot system for cooperative autonomous missions to secure airspace. We developed and integrated multi-modal perception using LiDAR, stereo camera, radar, and mono camera as sensors for detecting multirotor UAVs. We conducted extensive field tests and show that the proposed system is a suitable solution for long-term C-UAS operations with close-range air-to-air inspection and safe mitigation of intruders.

The positive results of this study allow for future research that can investigate the scaled system with multiple agents of each type. We will continue to improve the range and speed limits of our systems by investigating new hardware options and optimizing the developed algorithms.

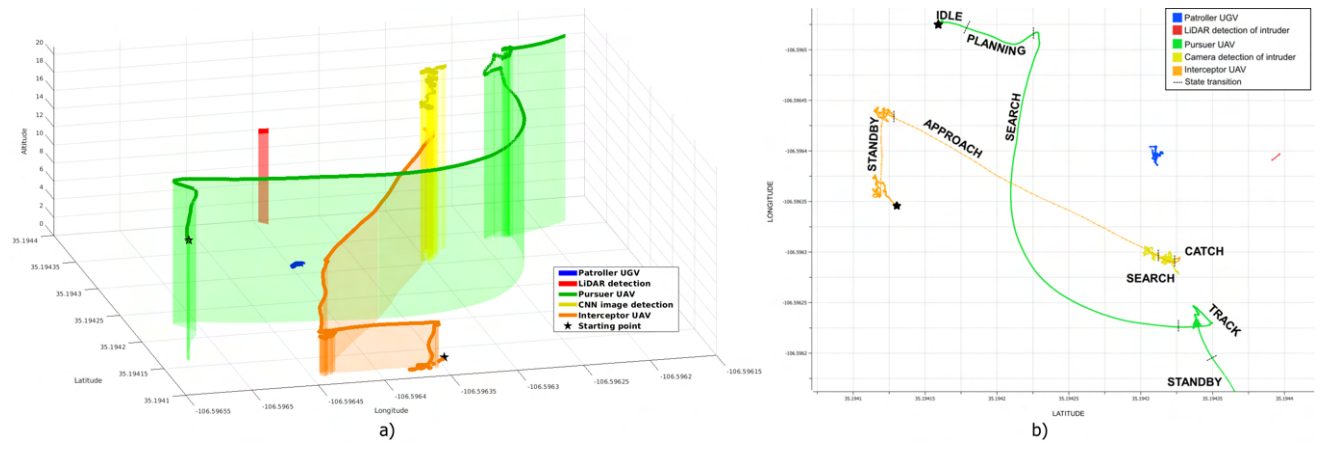


Fig. 10: Cooperative end-to-end mission in field experiments of a heterogeneous autonomous multi-robot system. The left image shows a 3D view, the right image a top-down view. The trajectories of the cooperative robots are reported by their GPS sensors, while the trajectory of the intruder is detected by multi-modal perception onboard the cooperative robots.

ACKNOWLEDGMENTS

We thank the Balloon Fiesta Park and the City of Albuquerque Parks & Recreation for their support. We thank John Ericksen for technical advice and assistance with the development of the UAV platform and GUI interface, and Jurica Goricanec for assistance with field experiments.

REFERENCES

- R. Mahony, V. Kumar, and P. Corke, "Multirotor aerial vehicles," *IEEE Robotics and Automation Magazine*, vol. 20, no. 32, 2012.
- [2] J. Ericksen, G. M. Fricke, S. Nowicki, T. P. Fischer, J. C. Hayes, K. Rosenberger, S. R. Wolf, R. Fierro, and M. E. Moses, "Aerial survey robotics in extreme environments: Mapping volcanic CO₂ emissions with flocking UAVs," *Frontiers in Control Engineering*, vol. 3, pp. 1– 13, March 2002.
- [3] J. Wang, Y. Liu, and H. Song, "Counter-unmanned aircraft system (s)(C-UAS): State of the art, challenges, and future trends," *IEEE Aerospace and Electronic Systems Magazine*, vol. 36, no. 3, pp. 4–29, 2021.
- [4] H. Kang, J. Joung, J. Kim, J. Kang, and Y. S. Cho, "Protect your sky: A survey of counter unmanned aerial vehicle systems," *IEEE Access*, vol. 8, pp. 168671–168710, 2020.
- [5] A. Barisic, M. Car, and S. Bogdan, "Vision-based system for a realtime detection and following of UAV," in 2019 Workshop on Research, Education and Development of Unmanned Aerial Systems (RED UAS), pp. 156–159, IEEE, 2019.
- [6] A. Barisic, F. Petric, and S. Bogdan, "Brain over brawn: Using a stereo camera to detect, track, and intercept a faster UAV by reconstructing the intruder's trajectory," *Field Robotics*, vol. 2, pp. 222–240, 2022.
- [7] M. Vrba and M. Saska, "Marker-less micro aerial vehicle detection and localization using convolutional neural networks," *IEEE Robotics* and Automation Letters, vol. 5, no. 2, pp. 2459–2466, 2020.
- [8] F. González, R. Caballero, F. J. Pérez-Grau, and A. Viguria, "Vision-based UAV detection for air-to-air neutralization," in 2021 IEEE International Symposium on Safety, Security, and Rescue Robotics (SSRR), pp. 236–241, IEEE, 2021.
- [9] M. Vrba, D. Heřt, and M. Saska, "Onboard marker-less detection and localization of non-cooperating drones for their safe interception by an autonomous aerial system," *IEEE Robotics and Automation Letters*, vol. 4, no. 4, pp. 3402–3409, 2019.
- [10] A. Barisic, F. Petric, and S. Bogdan, "Sim2Air-Synthetic aerial dataset for UAV monitoring," *IEEE Robotics and Automation Letters*, vol. 7, no. 2, pp. 3757–3764, 2022.
- [11] M. F. Al-Sa'd, A. Al-Ali, A. Mohamed, T. Khattab, and A. Erbad, "RF-based drone detection and identification using deep learning approaches: An initiative towards a large open source drone database," Future Generation Computer Systems, vol. 100, pp. 86–97, 2019.
- [12] K. Paschalidis, O. Yakimenko, and R. Cristi, "Feasibility of using 360° LiDAR in C-sUAS missions," in *IEEE 17th International Conference* on Control & Automation (ICCA), pp. 172–179, IEEE, 2022.
- [13] V. U. Castrillo, A. Manco, D. Pascarella, and G. Gigante, "A review of counter-UAS technologies for cooperative defensive teams of drones," *Drones*, vol. 6, no. 3, pp. 1–36, 2022.

- [14] N. Souli, R. Makrigiorgis, A. Anastasiou, A. Zacharia, P. Petrides, A. Lazanas, P. Valianti, P. Kolios, and G. Ellinas, "HorizonBlock: Implementation of an autonomous counter-drone system," in 2020 International Conference on Unmanned Aircraft Systems (ICUAS), IEEE, sep 2020.
- [15] A. P. Vinod, B. HomChaudhuri, C. Hintz, A. Parikh, S. P. Buerger, M. M. Oishi, G. Brunson, S. Ahmad, and R. Fierro, "Multiple pursuerbased intercept via forward stochastic reachability," in *American Control Conference (ACC)*, pp. 1559–1566, IEEE, 2018.
- [16] P. M. Wyder, Y.-S. Chen, A. J. Lasrado, R. J. Pelles, R. Kwiatkowski, E. O. Comas, R. Kennedy, A. Mangla, Z. Huang, X. Hu, Z. Xiong, T. Aharoni, T.-C. Chuang, and H. Lipson, "Autonomous drone hunter operating by deep learning and all-onboard computations in gps-denied environments," *PLoS ONE*, vol. 14, no. 11, pp. 1–18, 2019.
- [17] K. Klausen, T. I. Fossen, and T. A. Johansen, "Autonomous recovery of a fixed-wing UAV using a net suspended by two multirotor UAVs," *Journal of Field Robotics*, vol. 35, no. 5, pp. 717–731, 2018.
- [18] J. Rothe, M. Strohmeier, and S. Montenegro, "A concept for catching drones with a net carried by cooperative UAVs," in 2019 IEEE International Symposium on Safety, Security, and Rescue Robotics (SSRR), pp. 126–132, IEEE, 2019.
- [19] M. Vrba, Y. Stasinchuk, T. Báča, V. Spurný, M. Petrlík, D. Heřt, D. Žaitlík, and M. Saska, "Autonomous capture of agile flying objects using UAVs: The MBZIRC 2020 challenge," *Robotics and Autonomous Systems*, vol. 149, pp. 1–13, 2022.
- [20] J. M. Goppert, A. R. Wagoner, D. K. Schrader, S. Ghose, Y. Kim, S. Park, M. Gomez, E. T. Matson, and M. J. Hopmeier, "Realization of an autonomous, air-to-air counter unmanned aerial system (CUAS)," in *First IEEE International Conference on Robotic Computing (IRC)*, pp. 235–240, 2017.
- [21] F. Chance, C. Little, M. McKenzie, R. Dellana, D. Small, T. Gayle, and D. Novick, "Biologically inspired interception on an unmanned system.," tech. rep., Sandia National Labs, Albuquerque, NM, USA, 2021
- [22] F. Chance, "Lessons from a Dragonfly's brain," IEEE Spectrum, vol. 58, no. 8, pp. 28–33, 2021.
- [23] M. R. Brust, G. Danoy, D. H. Stolfi, and P. Bouvry, "Swarm-based counter UAV defense system," *Discover Internet of Things*, vol. 1, no. 2, pp. 1–19, 2021.
- [24] I. Yadav and H. G. Tanner, "Mobile radiation source interception by aerial robot swarms," in 2019 International Symposium on Multi-Robot and Multi-Agent Systems (MRS), pp. 63–69, IEEE, 2019.
- [25] "Classification of the unmanned aerial systems." https://www.e-education.psu.edu/geog892/node/5, 2022. Accessed: 2022-07-07.
- [26] G. Lykou, D. Moustakas, and D. Gritzalis, "Defending airports from UAS: A survey on cyber-attacks and counter-drone sensing technologies," *Sensors*, vol. 20, p. 3537, jun 2020.
- [27] H. Pham and Q.-C. Pham, "A new approach to time-optimal path parameterization based on reachability analysis," *IEEE Transactions* on *Robotics*, vol. 34, pp. 645–659, jun 2018.